# TUNING AND AUTOMATIC PHASE ADJUSTMENT IN EXTERNAL CAVITY DIODE LASER BEAM COMBINERS

Final Report



Prepared by

Dr. Roger S. Putnam
Aerodyne Research, Inc.
45 Manning Road
Billerica, MA 01821

Prepared for

Dr. Herschel Pilloff
Office of Naval Research
800 North Quincy Street
Arlington, Virginia 22217

Prepared Under Contract No.
N00014-91-C-0025



February 1992

ABSTRACT

We report quantitative measurements of self correcting phase shift produced in phaselocked beam combiners using multiple antireflection coated diode lasers in an external cavity. The major result is the demonstration that the primary automatic phase adjustment is produced by optical frequency changes acting on the difference in pathlengths to the individual diode lasers, and that secondary phase changes are produced by fluctuations of the internal optical power acting on any imbalance among the various diode lasers' saturation behaviors.

This suggests that the worst condition for a beam combining external cavity using automatic phaselocking is a near perfect pathlength match of the multiple laser arms. Further, the dynamic instability of a two laser system is measured and shown to be at its worst as the cavity length mismatch approaches zero. A second demonstration is controlled tuning over a frequency range corresponding to the inverse of the cavity length difference by piezo control of the phase error. Finally, the advantage for automatic phaselocking of using geometrically increasing feed lengths for the various diode lasers in the cavity is modeled and demonstrated.

TABLE OF CONTENTS

# 1. INTRODUCTION

Several techniques have been demonstrated for coherent beam combining including intracavity beamsplitters,[1] phase conjugate systems,[2] proximity or evanescent wave coupling,[3] intracavity holographic mode matching,[4] scraper mirror mode matching,[5] and intracavity fourier plane spatial filters.[6,7] All of these systems have some kind of beam combining arrangement and a phaselocking mechanism. In some cases the beam combiner works whether or not the beams are properly phases, such as scraper mirror; though most systems demand proper phaselocking, for example when a beamsplitter is used backwards as a beam combiner. Phaselocking can be enforced by injection from a separate master oscillator, encouraged by mutual injection, or demanded by intracavity filters that produce large losses for mutually incoherent fields.

The beam combining concept seeks to collect more power from multiple lasers rather than from scaling up a single laser. The techniques listed above are all amenable to diode lasers, and three of them are quite similar. These systems use intracavity spatial filters, holograms, or beamsplitters. The operation of these three beam combining techniques are similar in that large intracavity losses occur if the various gain arms (lasers) do not contribute the correct optical frequency and phase, and that the mathematics governing the phaselocking behavior is essentially the same. We chose to work with the beamsplitter system (Michelson cavity) shown conceptually in Figure 1 because we consider it easier to understand, to build, model, and to test, as it is an archetypical design with a minimum of distractions.

The Michelson cavity or beamsplitter of Figure 1 has two gain cells with separate mirrors in two arms at one end of the cavity, and a second laser mirror at the common end of the cavity. Blocking one gain arm permits the other gain cell to lase using the common mirror though with a large loss due

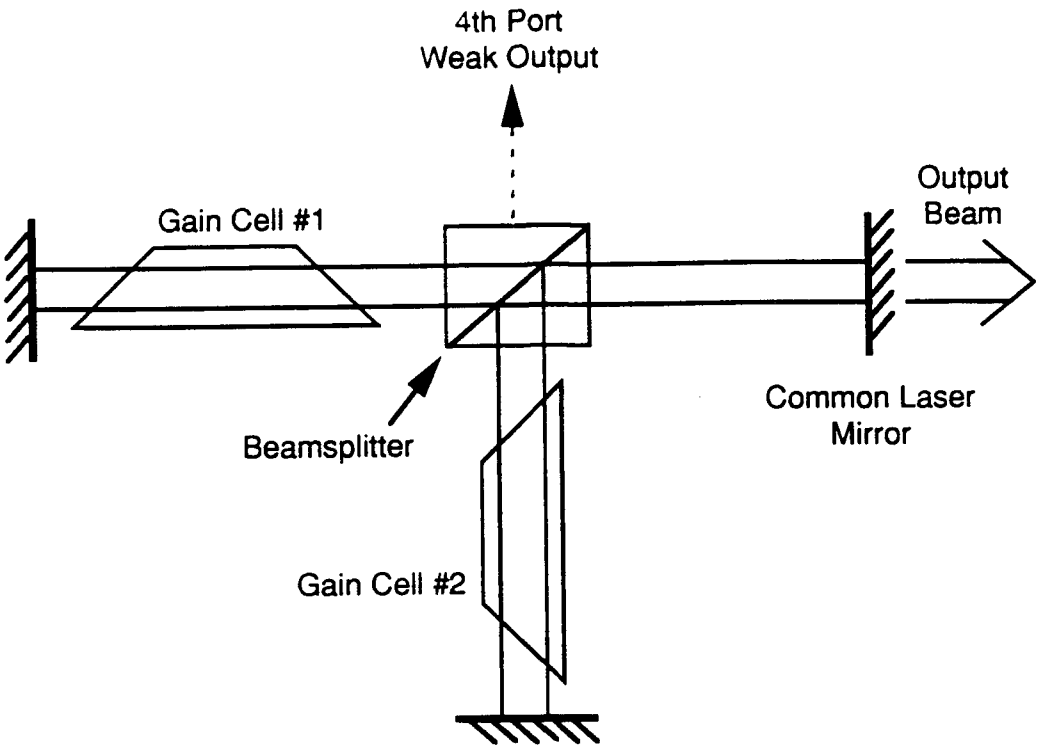


Figure 1. The Two Gain Arms Lase Using Their Individual Mirrors and the Common Mirror at the Right. The intracavity beamsplitter produces a large loss unless the fields emerging from the gain cells and entering the beamsplitter are phased to cancel at the fourth port and to thereby reach the common laser mirror unattenuated.

to two passes through the 50/50 beamsplitter. With both gain arms operating the beamsplitter will send all the energy to the common mirror if the fields entering the beamsplitter from the gain cells are phased correctly, cancelling the output from the (upper) fourth port of the beamsplitter. The optical gain required for lasing by each gain cell decreases by a factor of four if the contributions from the two gain arms are mutually coherent and phased correctly. More gain cells can be added using more beamsplitters in a tree structure, with a greatly increased loss to any gain cell that lases independently. The excess gain needed for lasing by an independent gain arm is $N^2$ for an N laser system.

Multiple lasers can be included without a tree structure of 50/50 beamsplitters by using some kind of multiport coupler such as a fiber

N-splitter, a (holographic) phase grating as used by Leger,[4] or an (comb filter) amplitude grating used by Philipp-Rutz[6] and Rediker.[7] The grating designs generate separate beams in an angular fan, which can be highly efficient if a thick hologram is used. An amplitude-only grating cannot be made 100% efficient for dispersing a TEMoo beam, and therefore this design requires that a more complicated beam structure exist at the common mirror end of the cavity. These grating based multiport beam combiners are intrinsically wavelength sensitive, not through direct attenuation which is an insignificant effect here but by misalignment of the beams which are focused back into the diode lasers' apertures.[8]

A similar and widespread technique is the use of a pinhole at a laser cavity beam waist for mode control. In essence the different (transverse) parts of the gain medium can act as separate gain arms and the pinhole produces loss unless all the sectors of the optical beam converging to the pinhole have the same phase. Opening up the pinhole from the diffraction limit decreases the coupling from 100% mix across the converging beam to any degree of nearest neighbor overlap. A somewhat similar concept has been applied to an array of diode lasers by using a diffractive microlens array to directly collimate the individual expanding beams as they emerge from the diode lasers.[9] The beams are 50 μm by 69 μm, essentially fully packed, and initially collimated. A flat common mirror provides feedback, and its spacing from the lenslet array decides the degree of coupling from nearest neighbor (small spacing) to fully mixed. The reflected light is reimaged despite diffraction of the nonuniform beam because of the Talbot effect which occurs for periodic sources[10] which are properly phaselocked.

## 2. THE TUNABLE MICHELSON LASER USING INTRACAVITY BEAMSPLITTERS AND MULTIPLE GAIN CELLS

The Michelson laser as shown in Figure 1 was conceived as a technique to obtain high gain and output power from a long gas laser without mode hopping despite the close mode spacing.[1] In this design the two cavities formed by the individual gain arms and the common mirror had slightly different lengths to permit lasing at only those frequencies where the difference in the round trip pathlength was an integer number of whole cycles. The effect is visible in Figure 1 by observing that the optical field returning from the common mirror enters the beamsplitter, feeds into the two gain arms and returns to add or cancel in the beamsplitter depending on the difference in the round trip pathlength. A small pathlength difference produces a cyclical gain function but one which is much broader than the longitudinal mode spacing for the long cavity. The system does tune using piezo controllers with smooth tuning when driving the common mirror and mode stepping when using one mirror on either gain arm.[1]

The Michelson laser tuning technique has recently been applied at 1300 and 1500 nm using a fully integrated pair of lasers and a y-coupler.[11] Current control individually adjusts optical lengths in the lasers, the y-coupler, and the end mirror waveguide. The result is smooth tuning over 2 nm sections and an overall tuning range of 22 nm.

Our re-invention of the multilaser beamsplitter cavity results from identifying and modeling how differences in the pathlengths of the various gain arms in beam combiners will increase the probability that an optical frequency exists where all the differences in pathlengths are approximately an integer number of wavelengths. Thus large pathlength differences may randomly permit lasing in a beam combining laser cavity without active cavity length control. It is also evident that given imperfectly phased cavity lengths, a near match would be the worst condition. We will elaborate on this issue in the section on Tuning Behavior.

# 3. THRESHOLD BEHAVIOR OF THE MICHELSON LASER CAVITY USING TWO AND THREE DIODE LASERS

## Laser Diodes

The three diode lasers employed in the subsequent experiments were Sharp LT024MD devices with free lasing wavelengths within 1 nm of 782 nm. These devices have a sapphire pseudo antireflection coating in the vicinity of 1% reflectivity on the output facet and a high reflectivity dielectric coating on the other facet. A D.O. Industries collimating lens and mount (#1-9101) were used which provided a 4.9 by 2.2 mm beam. The far field is double lobed with phase inversion across the beam, which requires attention during the alignment of the interferometric multi laser system.

## Laser Characterization

The three lasers were individually characterized in a one meter external cavity using a high reflector end mirror and a convenient two lens telescope adjusted to minimize the lasing threshold. Introducing neutral density filters inside the cavity and measuring the lasing threshold currents yielded the gain versus current curves shown in Figure 2. The slopes are 1.5-1.7 dB/mA.

## Temperature Tuning

The temperature tuning rate of the bare lasers was measured using a monochromator and 0.1°C temperature control was provided. A 5°C change causes a shift of one longitudinal mode of the partially antireflection coated lasers, and the temperatures were adjusted initially to approximately overlap these modes under operating conditions. The laser temperatures were not repeatedly optimized despite some tuning[12] which takes place due to changes in

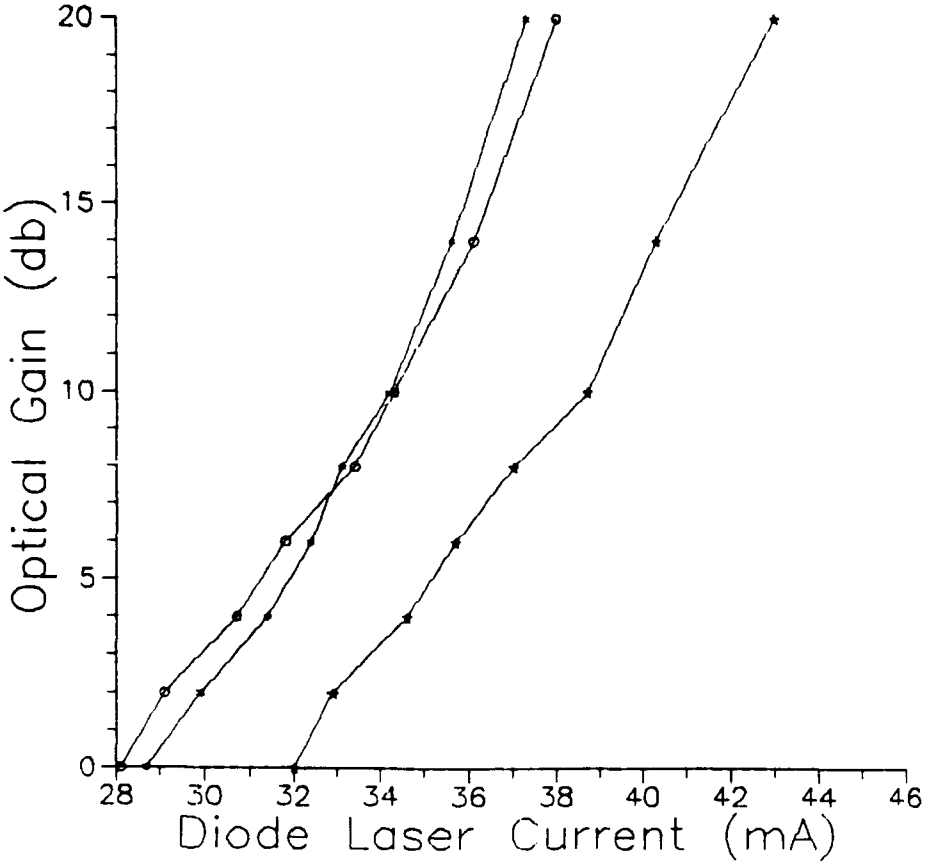


Figure 2. The Optical Gain of the Three AR Coated Diode Lasers was Measured by Introducing Neutral Density Filters Into an External Cavity and Observing the Lasing Current Threshold. The slopes range from 1.5 to 1.7 dB/ma (Asterisks: Laser #1; Stars: #2; Circles: #3).

diode gain (electron density) produced in these interferometric cavities which have dynamically varying optical losses.

Two Diode Lasers Phaselocked in the Beamsplitter Cavity

Figure 3 shows a simplified diagram of the two-laser experiments. The lasing threshold current increases by over 3 mA for each diode if one gain arm is blocked, implying an increased optical gain of about 5 dB. The theoretical increase is 6 dB from two passes through the 50/50 beamsplitter without an equal phaselocked contribution from the blocked gain arm.

Figure 4 shows the tradeoff in laser currents required to reach lasing threshold. Overlaid is the result of our model of the two laser threshold currents.

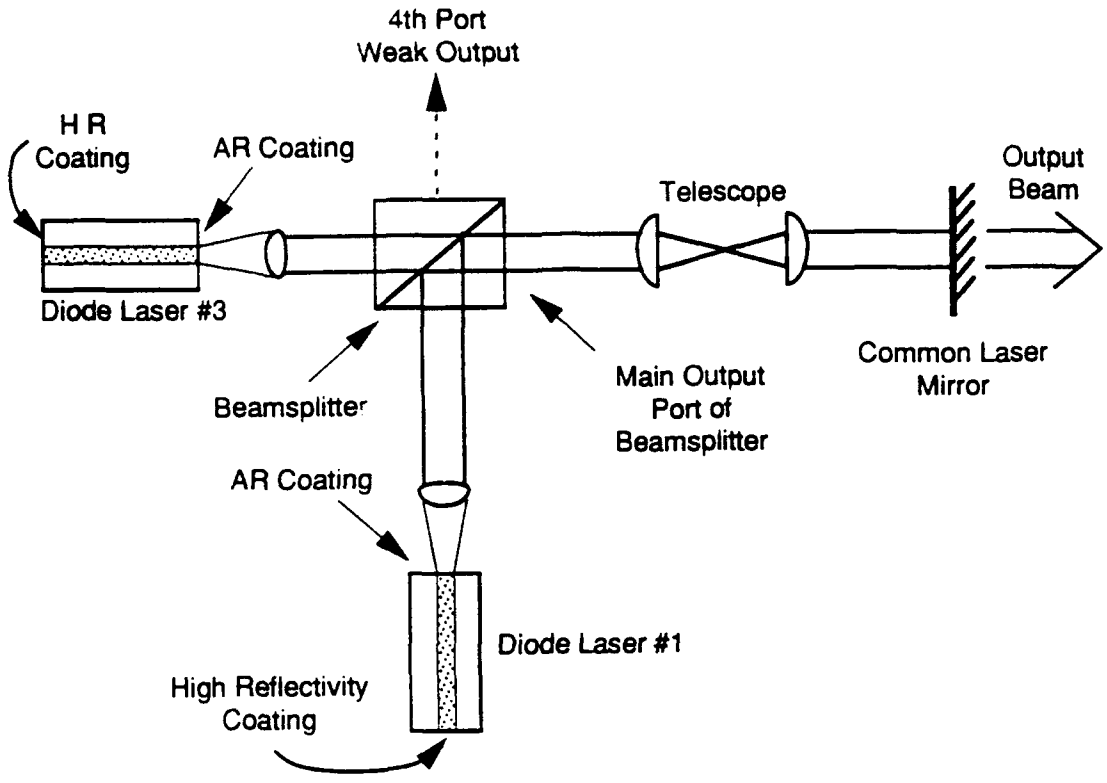


Figure 3. The Two AR Coated Diode Lasers Utilize the Common Mirror at the Right for Lasing. The optical field returning from the common mirror is amplified by both diode laser gain cells and is recombined at the beamsplitter. Lower cavity losses result for properly phased optical fields. The fractonal output at the 4th port of the beamsplitter increases for amplitude or phase mismatches in the recombining beams.

Model of the Two Laser Threshold Currents

The empirical diode laser gain model is:

$$\text{Power Gain} \quad G = e^{k(i-i_o)} - ca$$

where:

i is the diode laser current

$i_o$ is a device constant, which we determine by the cavity loss and solo lasing threshold

a is the diode output flux (in mW)

c is a constant based on the differential efficiency (mW/mA) of the bare diode $c = k/(df/di)$

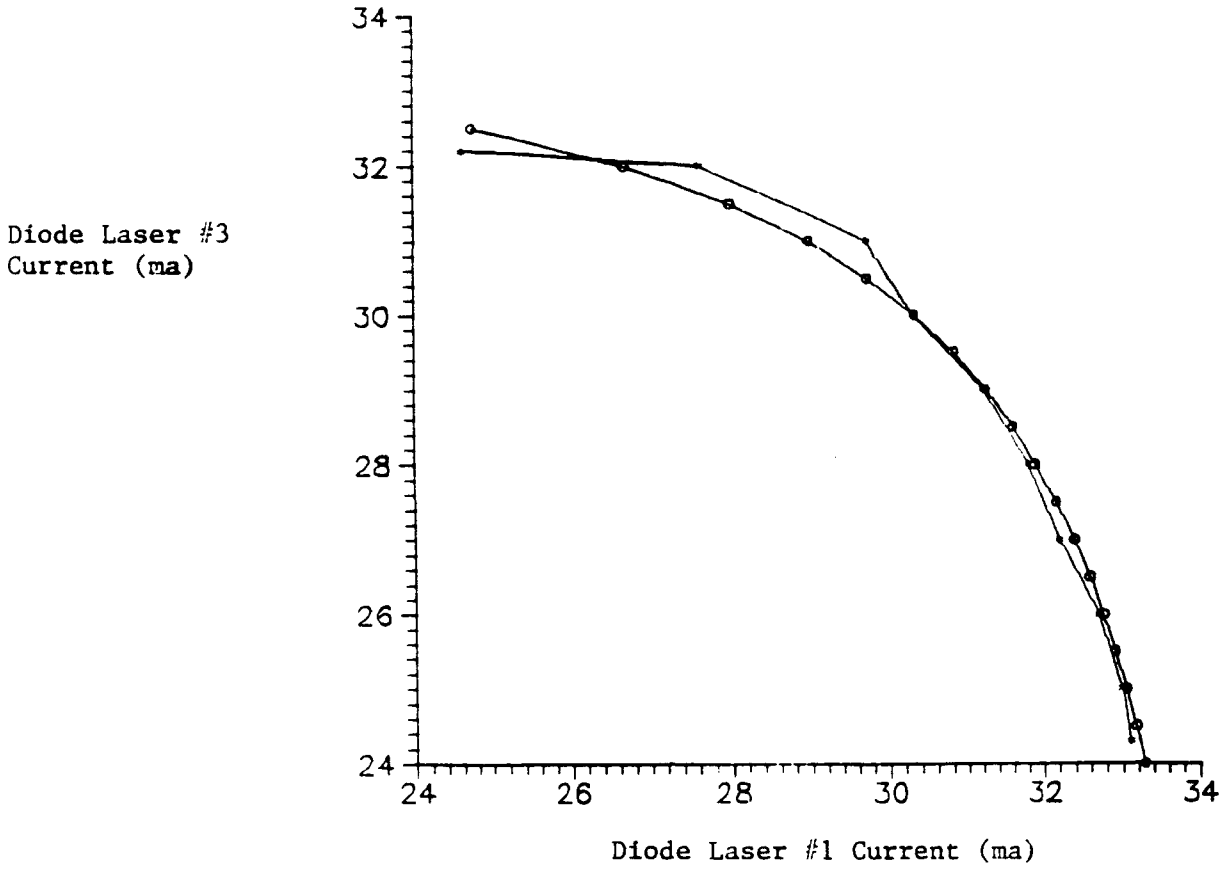


Figure 4. The Measured (Asterisks) Diode Currents Required to Achieve Lasing Threshold in the Two Laser Cavity Show an Expected Tradeoff Eventually Limited by One Diode Lasing Independently of the Other Gain Arm Despite the High Round Trip Loss in the Beamsplitter. The model (circles) of the threshold currents is based on the measured gain vs. current rate and the lasing thresholds of each laser with the other gain arm blocked.

The cavity gain requirement is:

$(\sqrt{G_1/2} + \sqrt{G_3/2})^2 = 2/R$ :assuming perfect phasematch and perfect beam overlap

Where $G_1$, $G_3$ are the laser gains, and R is the common mirror reflectivity (which includes other cavity losses other than the beamsplitter).

Figure 4 shows the result of the model using threshold currents for each laser operating alone and with no fitted parameters.

Power Collection Efficiency at the Beamsplitter

The power collection efficiency was obtained by measuring the optical power emitted out the upper (fourth) port of the beamsplitter as shown in Figure 3. This port ideally gives zero output for perfectly phaselocked input beams, assuming equal power and a perfect beam overlap.

Figure 5 gives the ratio of power emitted at the "cancelled" fourth port to that of the desired main port feeding the common mirror. The horizontal axis is the laser diode current difference ($I_1$-$I_3$) with a fixed $I_1 + I_3$ (equal to 2 and 4 ma above the collective threshold for the asterisk curves). The open circle curve is a simple model of the upper data curve.

The Ratio reaches 1.0 if one gain arm is blocked as expected from the 50/50 beamsplitter. Diode laser current imbalance leads to an imbalance in the contributed optical powers and incomplete cancellation at the fourth port of the beamsplitter. The Ratio approaches but does not reach zero when balanced, and this is attributed to and modeled as incomplete beam overlap in the beamsplitter. A 92.3% beam overlap fits the data.

The minimum is observed to occur with a current imbalance of about 1.5 ma which we expect reflects differences in diode lasers #1 and #3, as well as imperfect beam division by the beamsplitter and other unbalanced optical losses.

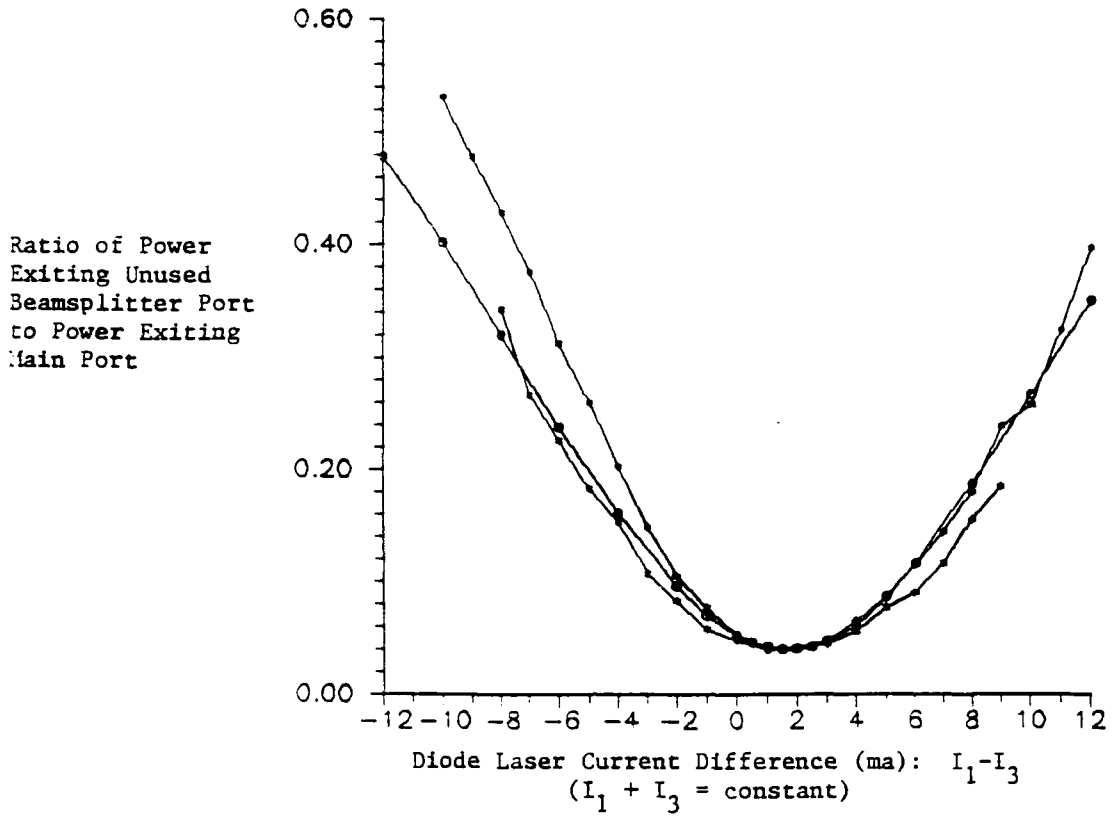


Figure 5. Under Perfect Matching of Amplitude and Phase and Beam Alignment, the Ratio Would be Zero with Perfect Cancellation at the Unused Beamsplitter Port. The ratio reaches 1.0 with one gain arm blocked. Unbalanced gain due to a diode drive current imbalance increases the ratio. The asterisk curves give experimental data for $I_1 + I_3 = 2$ or 4 ma above the collective threshold currents. The circles represent our model of the upper data curve.

Power Collection Efficiency Model

The new cavity gain equation employing the fractional beam overlap parameter f [0-1] is:

$$f \cdot (\sqrt{G_1} + \sqrt{G_3})^2 + (1-f) \cdot (G_1 + G_3) = 4/R \quad \text{(assumes perfect phase)}$$

This modification of the model gives the open circle curve shown in Figure 5. Fitting the curve to the experimental data at the minimum gives f = 0.923 for a 0.04 Ratio.

## 3. THREE DIODE LASERS PHASELOCKED IN A BEAMSPLITTER CAVITY

Figure 6 shows the cavity arrangement using one 50/50 beamsplitter and one 67/33 beamsplitter to provide a balanced three-way split. Figure 7 shows the measured tradeoff of the three diode laser currents required to reach lasing threshold.

### Multiple Phaselocked Laser Gain Model

For an N-port optical power splitter and N gain arms with gains $G_i$. The common mirror reflectivity = R (includes other cavity losses).

$$\left(\sum_{i=1}^{N} \sqrt{\frac{G_i}{N}}\right)^2 = \frac{N}{R}$$

or

$$\left(\sum_{i=1}^{N} \sqrt{G_i}\right)^2 = \frac{N^2}{R}$$

if $G_i = G$ then $G = \frac{1}{R}$

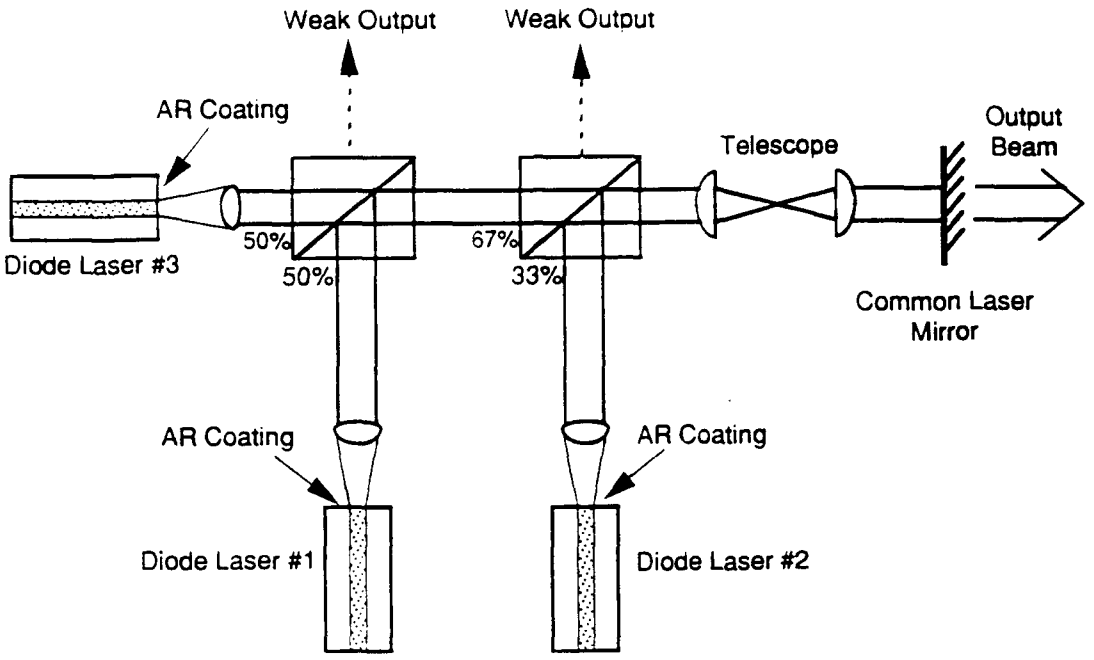


Figure 6. The Phaselocked Three Laser Demonstration Used Two Beamsplitters Arranged to Give an Equal 3-Port Power Division

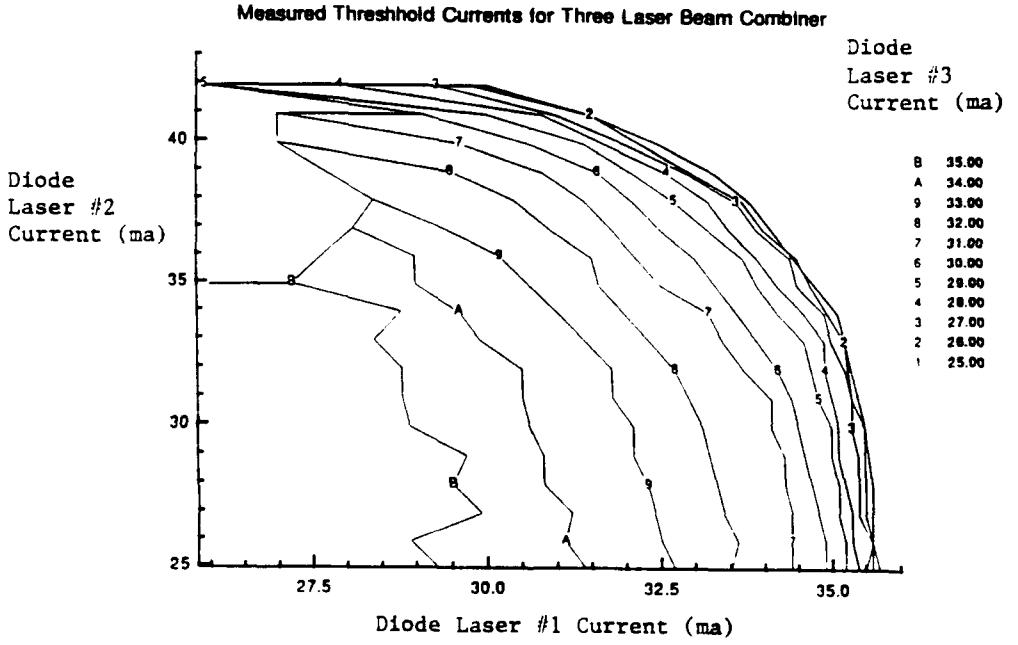


Figure 7. The Measured Diode Laser Currents for the Phaselocked Three Laser Demonstration is Shown as a Set of Contour Lines for Fixed Values of the Laser #3 Drive Current. The expected set of curves is similar to a two laser threshold curve with a bunching where the Laser #3 current is low enough to become irrelevant.

# 4. TUNING BEHAVIOR

The original motivation for using the two laser Michelson cavity was it's step tuning by longitudinal modes across the whole gain bandwidth of a gas laser with smooth tuning available between steps.[1] Our motivation with this cavity design is for both the intentional tuning ability afforded multilaser beam combiners and the unintentional tuning ability which keeps the output power high despite phase errors in the system.

The primary tuning feature of the Michelson Laser Cavity as shown in Figure 1 is produced by the difference in pathlengths in the two gain arms. This path difference can be short and produce a broad tuning shape that allows lasing at only one longitudinal mode of a long laser cavity. This path difference can also be made very large to ensure that there will always be some frequency at which lasing can occur despite drift in the cavity lengths.

## Mode Location and Power Collection Efficiency in the Two Laser Cavity

The modes of the combined cavity are generally shifted from the longitudinal modes of the two separated cavities which consist of the common mirror and each individual gain arm. The new mode locations are shown in Figure 8. The location of a combined cavity mode requires that the phase errors produced at this new frequency by one round trip in the separated cavities be equal and opposite ($\phi_a = -\phi_b$), and less than $\pm 90°$. There is a $360°$ round trip phase shift in moving from one mode to the next in each separated cavity. Equal and opposite phases ensures a whole number of cycles in one round trip, assuming balanced amplitudes emerging from the two gain arms. However, not every new cavity mode corresponds to a peak in power combining efficiency at the beamsplitter which occur for $\phi_a = \phi_b$ as shown in Figure 9.

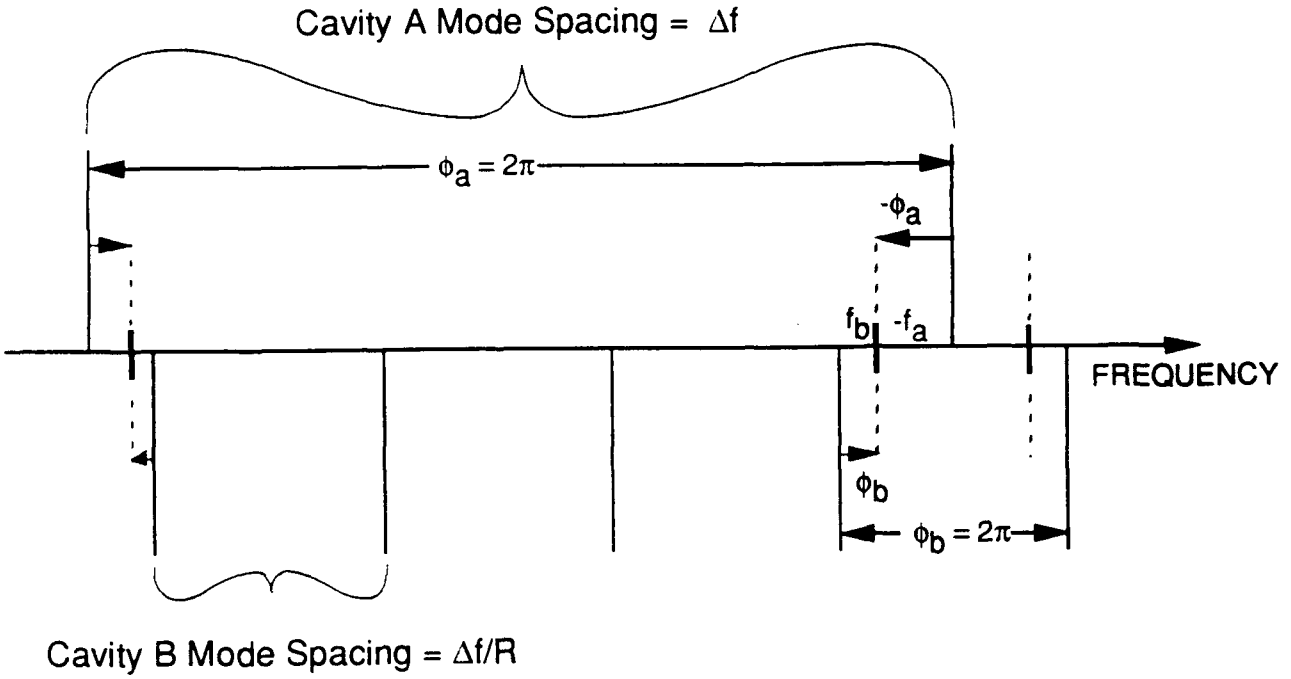


Figure 8. The Modes of Two Separated Cavities and the New Mode Locations in a Beam Combiner with a Length Ratio of R are Depicted. For equal amplitudes the phase errors produced by each cavity at the new mode frequency must be equal and opposite and less than $\pm 90°$ ($\phi_a = -\phi_b$) to have an integral number of cycles fit in one round trip in the combined cavity. These new modes can be very lossy. (we have absorbed the fundamental beamsplitter phase shift into the cavities)

From Figure 8:

$-f_a + f_b = \Delta f/2R$ : Worst case has Cavity A mode location midway between two modes of Cavity B. $f_a$, $f_b$ are frequency shifts from separated cavity modes to the new combined cavity mode

$$-\frac{\phi_a}{2\pi} \cdot \Delta f + \frac{\phi_b}{2\pi} \cdot \frac{\Delta f}{R} = \Delta f/2R$$ : 360° is a shift of one mode

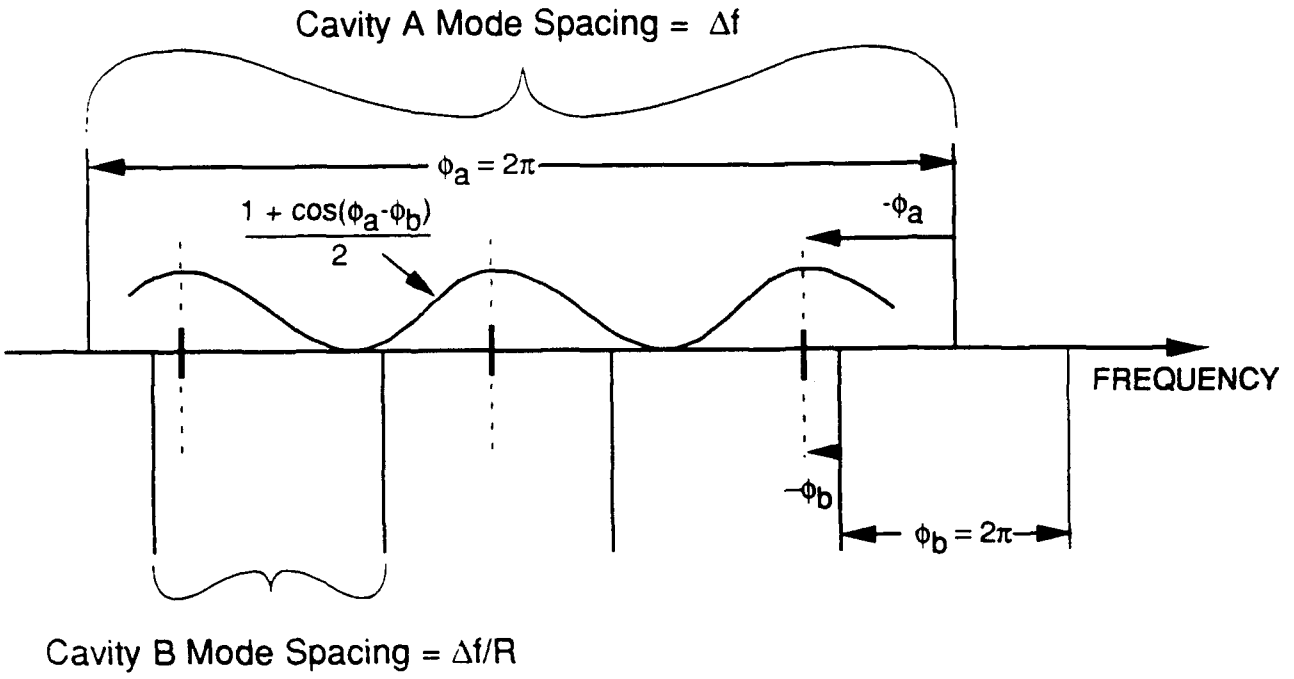


M91-310b/R.P.

Figure 9. The Beamsplitter Collects Power Efficiently for a Proper Phase Match Which is $\phi_a = \phi_b$. (We have absorbed the fundamental beamsplitter phase shift into the cavities.) The peaks are shown but do not always coincide with mode locations of the combined cavity. The cosine function gives the power collection efficiency.

$\phi_a = -\phi_b$ , $|\phi_a, \phi_b| \leq \pi/2$ : Gives location of new mode with integer number of cycles in one round trip assuming equal amplitudes from both gain arms

$$-\frac{\phi_a}{2\pi}\left[1 + \frac{1}{R}\right] = \frac{1}{2R}$$

$\phi_a = -\pi/(R+1)$ , $\phi_b = \pi/(R+1)$ : Worst case phase shifts for cavity length ratio = R.

The power collection efficiency at the beamsplitter depends on the phase difference of the fields:

$$E_p = 1/4\ [(1 + \cos^2(\phi_b-\phi_a) + \sin^2(\phi_b-\phi_a)] = 1/2\ [1 + \cos(\phi_b-\phi_a)] \quad ,$$

with

$$\phi_b-\phi_a = 2\pi/(R+1) \quad .$$

Figure 10 shows the power collection efficiency at the beamsplitter versus the ratio of the two cavity lengths for the worst case phase adjustment. A large ratio for the cavity lengths ensures that there will always be a mode of the long cavity that is close to any given mode of the shorter cavity.

This behavior has been observed in our two laser cavity by changing the cavity ratio R from 3 to 5.4, and to 8.2. As the cavity length ratio increased, the amount of time the laser system was lasing also increased when tested by vibrating one gain arm through multiple cycles of phase shift. This behavior can be extended to several lasers in a beam combiner with geometrically increasing cavity lengths, providing efficient phaselocked performance by guaranteeing a nearby mode from each gain arm.

The tuning behavior of the Michelson Laser Cavity for fractionally different cavity lengths[1] is diagrammed in Figure 11. The arrows indicate the peaks of the cyclical collection efficiency based on the difference in pathlengths. The cavity can be tuned in steps by piezo control of one gain arm, pulling the frequency slightly from the indicated lasing frequency before jumping one mode of the unchanged gain arm. Lasing may fail due to inadequate gain between the mode hops. Continuous tuning[1] over a maximum of one mode spacing, depending on available gain, is available by piezo control of the common mirror. Smooth tuning should be possible over a much wider range if any two of the three mirrors are driven together in the proper ratio.

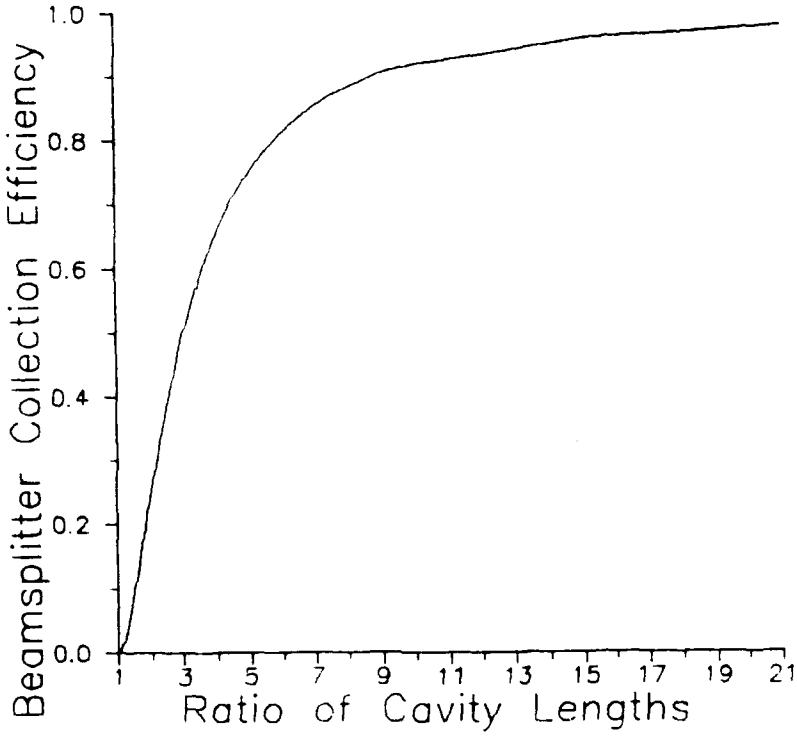


Figure 10. The Calculated Power Collection Efficiency of the Beamsplitter for a Two Laser System at the Worst Case Phase Condition Increases as the Ratio of the Two Cavity Lengths Increases

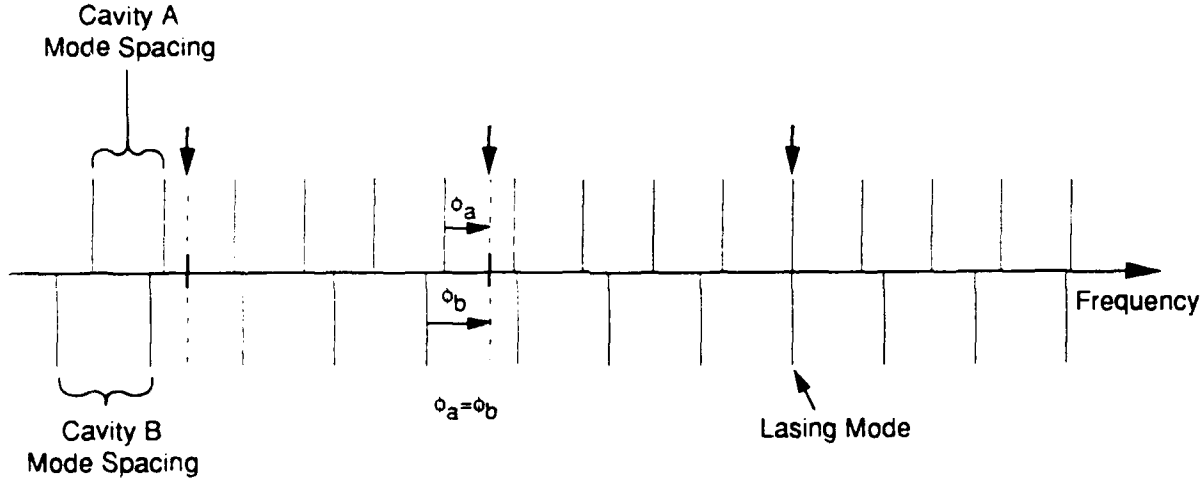


Figure 11. The Mode Location of a Two Laser Michelson Cavity with Fractionally Different Cavity Lengths is Shown with a Perfect Match at One Mode from Each Cavity. The arrows indicate areas of maximum power collection efficiency. Step tuning is available if one set of modes are shifted and continuous tuning is available if both sets are shifted.

## 5. MEASUREMENT OF THE INTERNAL PHASE SHIFTS PRODUCED BY CHANGES IN FREQUENCY AND AMPLITUDE

It is evident that a balanced Michelson Laser Cavity which has gain arms of nearly equal length will only lase if the modes of the two cavities happen to coincide. Here we test our theory that the ability of laser beam combiners to phaselock automatically depends on an imbalance in the lengths of the gain arms and on an imbalance in the saturation or gain behavior of the gain arms, and that the resulting phase shifts increase the likelihood of finding an in-phase condition for all the contributing gain cells.

### Phase Shifts Produced by Changes in Optical Amplitude

The beamsplitter cavity shown in Figure 3 was arranged with each separate round trip pathlength equal to 160 cm. This adjustment was made to an accuracy of a few microns by modulating the phase by vibration and minimizing the minimum laser output while using high gain from the AR coated diode lasers. This adjustment is based on the view that with balanced pathlength and gain conditions neither changes in optical frequency nor amplitude can produce a compensating differential phase shift between the gain arms, and therefore lasing can be forced to stop by modulating the phase even with high optical gains. Figure 12 shows the output from the two laser system versus cavity length mismatch using balanced diode laser currents. Using the several cycle phase vibrator gave the upper maximum output and the lower minimum output data.

The cavity lengths were adjusted to a zero mismatch and a calibrated linear phase shifter was constructed using a piezo driver. Figure 13 shows the laser output as a function of phase for three conditions of diode current balance. The sawtooth was adjusted to give 360° of roundtrip forced phase between the turnover points. The three curves consist of balanced diodes

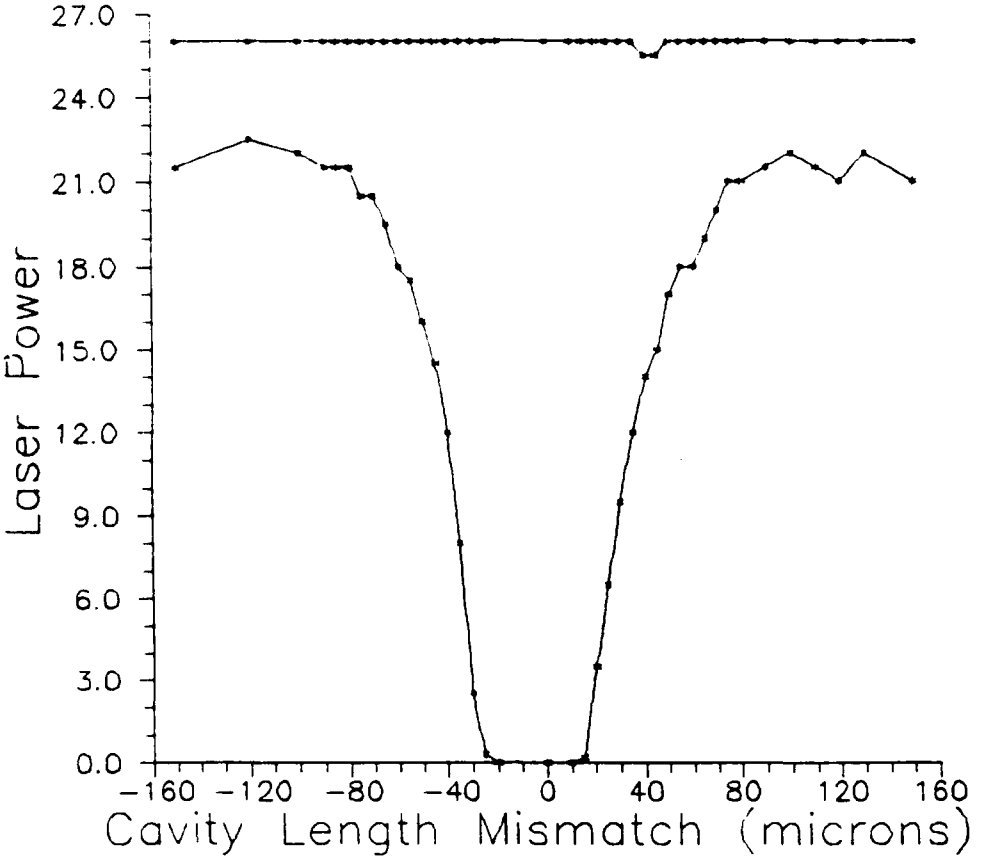


Figure 12. The Two Laser System Output Power is Shown for Best and Worst Phase Conditions as a Function of the Difference in the Two Cavity Lengths. For a matched condition, frequency changes cannot produce a correcting differential phase shift and the laser stops operating when the worst case phase shift puts the two cavities out of phase.

(middle) and $\pm 2$ ma unbalanced drives for the top and bottom curves showing opposite asymmetry. Under the assumption that frequency shifts are irrelevant with matched cavities, and that the remaining phase shift is due to differential changes in the diode's gain (electron density) due to different saturation behavior, we conclude that equal output powers occur for equal absolute phase errors in the beamsplitter. Thus by comparing the differences in the forced phase required to obtain the same amplitude we can extract the additional phase reaction of the system. Analyzing each of the three curves of Figure 13 separately gives the three curves of Figure 14. The curve with the balanced gain cells is centered and shows little differential phase reaction whereas current differences of $\pm 2$ ma give the other two curves with opposite polarity as expected.

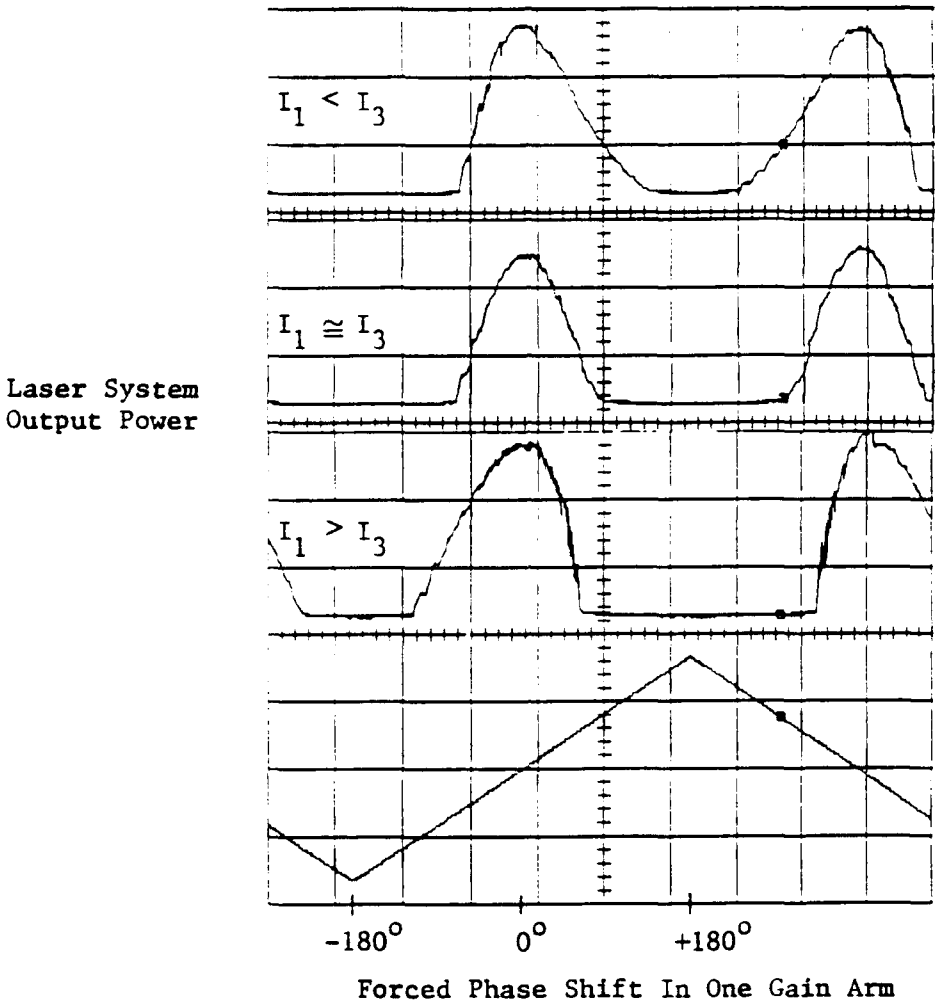


Figure 13. The System Output Power vs. a Forced Phase Shift in One Gain Arm Shows an Opposite Asymmetry for Laser Currents $I_1 < I_3$ and $I_1 > I_3$. This occurs for matched cavity lengths which prevents additional phase shifts based on frequency changes. The asymmetry is due to the imbalance in gain saturation which effects the optical indices in the diodes differently.

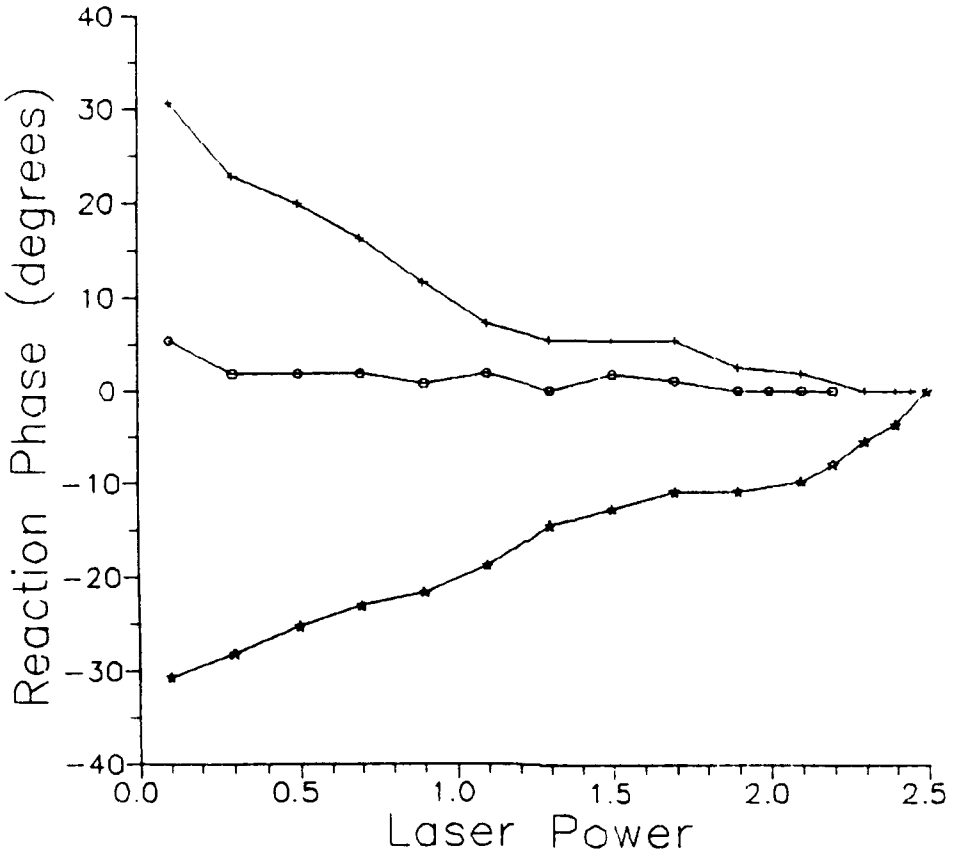


Figure 14. As the Internal Laser Power Decreases the Diodes' Saturation Changes and This Produces a Phase Shift in the Diodes. These phase shifts are not balanced if the diode drive currents are unbalanced, here by ±2 ma for the extreme curves. The center curve has balanced currents. These curves are derived from the laser amplitude versus forced phase experimental data.

Plotting the system's reaction phase shift versus the forced phase shift in Figure 15 is more revealing. The balanced gain case plotted with open circles shows small differential phase shifts as before. The upper curve shows a sharp rise in reaction phase when the forced phase shift is positive because the reaction phase shift is adding to the forced phase which increases the overall phase error. For a negative forced phase the reaction phase rises more slowly since it counteracts the forced phase error. The same effect is seen in the lower starred curve, though with the expected opposite behavior.

One result seen here is that the ±30° of reaction phase possible with imbalanced diode lasers is not adequate to compensate ±180° phase errors. Further the lasers do not always cooperate in these systems to reduce phase errors and can increase them. Finally, balanced diode laser saturation

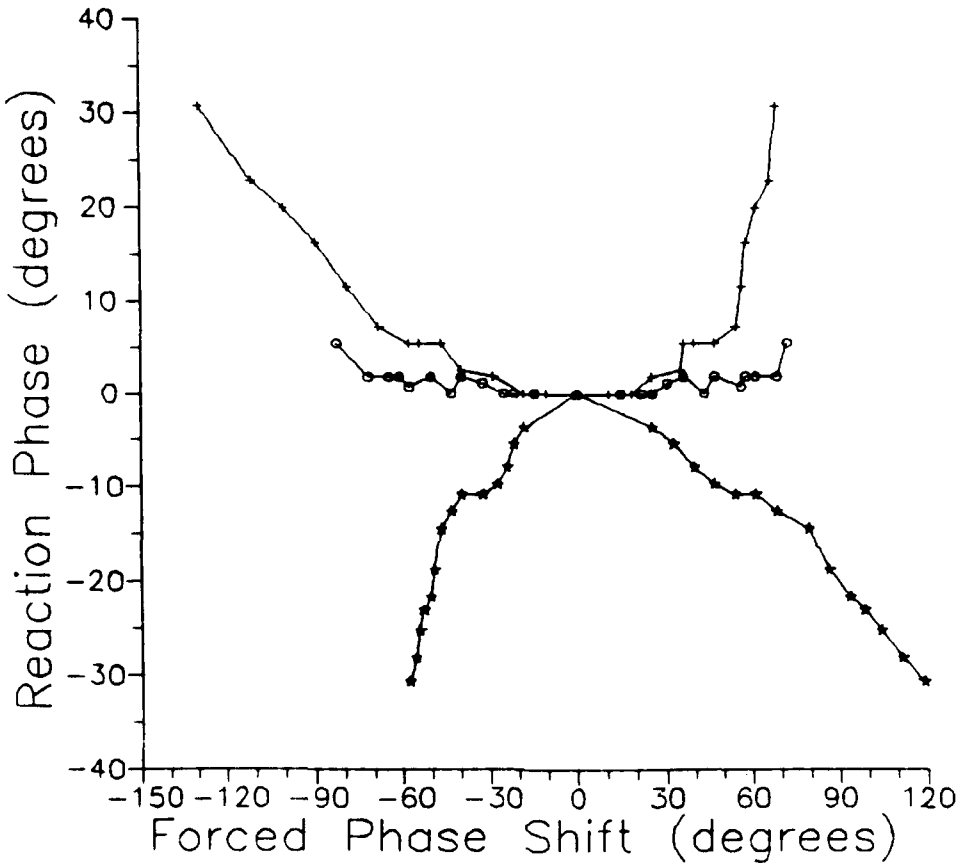


Figure 15. Measurement of the Reaction Phase of the Diode Lasers Due to Gain Saturation as a Function of the Forced Phase Shift in One Gain Arm. The two extreme curves correspond to unbalanced diode current drives (±2 ma). The middle curve was produced by balanced diode currents. The sharp rise in the upper right and lower left occurs because the reaction phase adds to the forced phase. This test was performed with equal cavity lengths to remove phase shifts due to frequency changes.

behavior will null out the reaction phase shift, which makes it a potential phase error correction mechanism of secondary importance. It does make a contribution to instability as is discussed later.

Phase Shifts Produced by Changes in Optical Frequency

Figure 12 gives the laser system output for best phase and worst phase conditions as a function of cavity length mismatch. If the increase in worst case output power with an increase in the cavity mismatch is due to frequency changes which produce phase error corrections then the width of the dip in Figure 12 should correspond to the gain bandwidth of the diode lasers. A measured

mismatch of 25 μm (50 μm roundtrip) produces ±180° with a ±6.4 nm shift at 800 nm which is a reasonable 1.6% bandwidth for a diode laser. The data supports the theory here.

Figure 12 gives the worst case output equal to about 85% of the best case output when frequency shifts are allowed to compensate phase errors. Using the following phase sensitive gain model of the cavity:

$$\left[\sqrt{G_1} + \sqrt{G_3} \cdot \cos(\theta)\right]^2 + \left[\sqrt{G_3} \cdot \sin(\theta)\right]^2 = 4/R$$

We obtain 85% output power with the same cavity losses and drive currents when we use a phase error of $\theta = \pm 30°$. Testing this model against the experimental data of laser output versus forced phase error shown in Figure 13 (middle curve with balanced diode currents) reveals a good match as shown in Figure 16.

We conclude that a reasonable experimental estimate of the residual phase error after automatic phase compensation by frequency changes in our phaselocked diode laser beam combiner is ±30°. We also conclude that frequency shifts acting on differences in pathlengths among the gain arms is the primary mechanism for automatic correction of phase errors in this class of beam combiners.

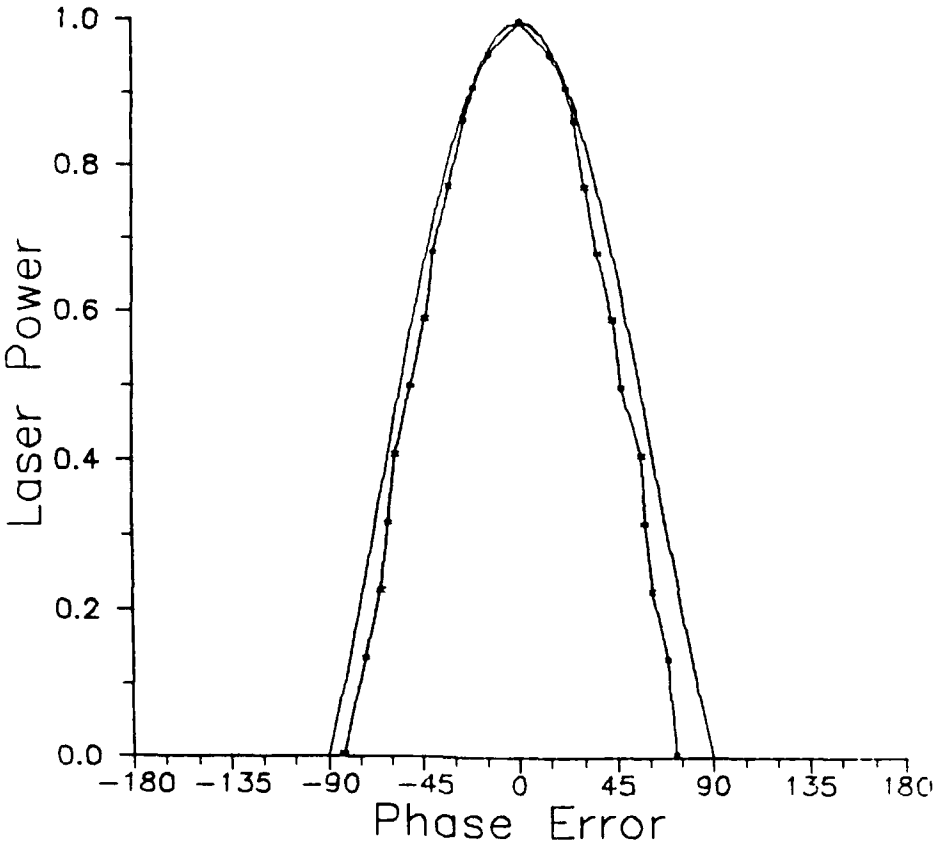


Figure 16. The Asterisks Show the Measured Output Power from the Two Laser Beam Combiner as a Function of Forced Phase Error. The diode drive currents are balanced and the cavity lengths are matched to minimize any reaction phase shift. The smooth curve is produced by our model which now includes phase errors at the beamsplitter.

## 6. MEASURED INSTABILITY AS A FUNCTION OF CAVITY LENGTH MISMATCH AND DIODE LASER CURRENT IMBALANCE

Instability and hysteresis is known to occur in laser systems due to feedback from a phase shift which induces an amplitude change, which in turn through gain saturation produces further phase shifts. This problem is accentuated in the two laser Michelson Cavity when the gain arm lengths are matched as shown in Figure 17. The two curves showing oscillation amplitudes are for two different diode current mismatch conditions. Thus the matched cavity condition which interferes with frequency shift induced phase compensation also corresponds to increased instability.

The effect of current imbalance has previously been shown to provide feedback in the form of a phase shift caused by unbalanced changes in gain saturation. Figure 18 shows that balancing the currents in the diode lasers will reduce the feedback which supports instability. The two gain arm lengths were equal for this demonstration.

We conclude that balancing the diode lasers' saturation behaviors in a phaselocked beam combiner reduces instability based on amplitude induced phase shifts; and that permitting frequency shifts to compensate phase errors through dissimilar cavity lengths will also reduce this instability.

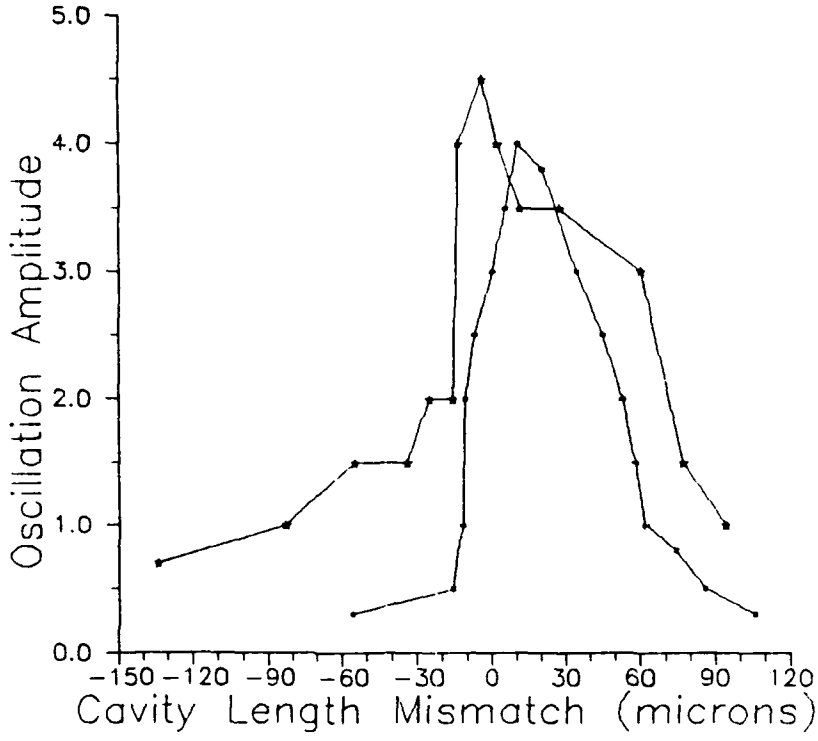


Figure 17. **Measuring High Frequency Jumps and Oscillations in the Optical Output Shows that a Perfect Cavity Match Significantly Increases the Instability. This test was performed with unbalanced diode laser currents.**

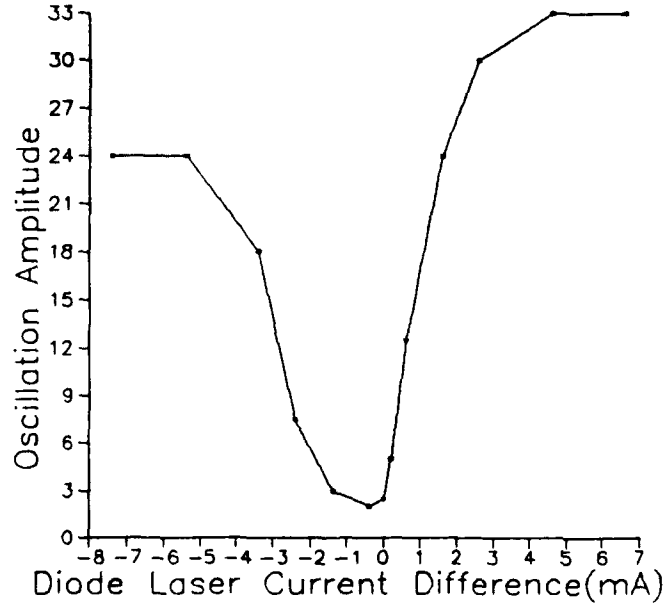


Figure 18. The High Frequency Jumps and Oscillation in the Optical Output are Shown to Decrease for Balanced Diode Laser Current Drives. This appears to be due to a reduction in feedback obtained by balancing the amplitude induced phase shifts. This test was performed with matched cavity gain arm lengths.

# 7. CONCLUSIONS

We have shown how phaselocked beam combining using intracavity holograms, spatial filters, or beamsplitters uses a similar multiport coupler which produces large optical losses if the contributed fields have incorrect phases; and that the existence of a phase correcting mechanism is necessary for sustained lasing, either an external active control or automatic frequency shifts operating through differences in gain arm pathlengths.

Our demonstrations involved an intracavity beamsplitter system which provided phaselocked operation for two and three diode lasers.

We have measured the phase shift produced individually by internal changes in optical amplitude and frequency in a diode laser beam combiner in response to intentional forced phase errors. Our results show that balancing the gain cells reduces the phase shifting reaction of the system to internal phase errors, but that this kind of reaction phase frequently exacerbates the original phase error and generally increases the instability. We have shown that frequency shifts are primarily responsible for the system's compensation of phase errors and that this occurs due to differences in pathlengths among the gain arms which produce differential phase shifts as the optical frequency changes. The worst case was shown to be a near perfect cavity length match for the gain arms which results in the laser stopping and starting with wavelength sized pathlength fluctuations. In addition, instabilities were most pronounced at a near perfect cavity length match.

We demonstrated the effectiveness of using widely different gain arm pathlengths in obtaining sustained lasing, and calculated the worst case phase error and beam combining efficiency of this free running system. We provided a simple interpretation of the system's mode locations as a function of the modes of the separated cavities which clearly predicts the tuning behavior

for systems with either large or small cavity mismatches. It was the broadband tuning ability which originally interested others in this Michelson Cavity Laser and it is this same tuning behavior which makes the automatic phase compensation in beam combiners possible.

We also demonstrated a simple model of the beamsplitter cavity for diode lasers which accurately predicted both the lasing threshold tradeoff of the two diode lasers' currents, and the power collection efficiency at the beamsplitter as a function of phase error and diode laser current imbalance.

## 8. REFERENCES


1. M. DiDomenico, Jr., "Characteristics of Single Frequency Michelson-Type He-Ne Gas Laser," IEEE J. Quant. Electron. QE-2, 311-322 (1966).

2. M. Cronin-Golomb, A. Yariv, and I. Ury, Appl. Phys. Lett. 48, 1240 (1986).

3. D.R. Scifres, R.D. Burnham, and W.S. Streifer, Appl. Phys. Lett. 41, 118 (1982).

4. J.R. Leger, G.J. Swanson, and W.B. Veldkamp, Appl. Phys. Lett. 48, 888 (1986).

5. G.E. Palma, W.J. Fader, and K.E. Oughstun, DTIC Technical Report, AFWL-TR-84-95 (1985).

6. E.M. Philipp-Rutz, Appl. Phys. Lett. 26, 475 (1975).

7. R.H. Rediker, R.P. Schloss, L.J. Van Ruyven, Appl. Phys. Lett. 46, 133 (1985).

8. R.H. Rediker, K.A. Rauschenbach, and R.P. Schloss, IEEE J. Quant. Elect. 27, 1582 (1991).

9. J.R. Leger, M.L. Scott, and W.B. Veldkamp, Appl. Phys. Lett. 52, 1771 (1988).

10. J.R. Leger and M.A. Snyder, Appl. Opt. 23, 1655 (1984).

11. M. Schilling, W. Idler, E. Kuhn, G. Laube, H. Schweizer, K. Wunstel, and O. Hildebrand, IEEE J. Quant. Elect. 27, 1616 (1991).

12. J. Manning, R. Olshansky, and C.B. Su, IEEE J. Quant. Elect. QE-19, 1525 (1983).